Detection of Essential Tremor at the S-Band

Yang, X., Shah, S., Ren, A., Fan, D., Zhao, N., Cao, D., Hu, F., Ur-Rehman, M., Wang, W., von Deneen, K. M. & Tian, J.

DOI 10.1109/JTEHM.2017.2789298
ISSN 2168-2372

Publisher: IEEE

IEEE Journal of Translational Engineering in Health and Medicine

Received 21 August 2017; revised 11 November 2017 and 15 December 2017; accepted 27 December 2017.
Date of publication 24 January 2018; date of current version 8 February 2018.

Digital Object Identifier 10.1109/JTEHM.2017.2789298

Detection of Essential Tremor at the *S*-Band

XIAODONG YANG[1], (Senior Member, IEEE), SYED AZIZ SHAH[2], AIFENG REN[1], DOU FAN[1], NAN ZHAO[1], DONGJIAN CAO[1], FANGMING HU[1], MASOOD UR REHMAN[3], (Senior Member, IEEE), WEIGANG WANG[4], KAREN M. VON DENEEN[5], AND JIE TIAN[5,6], (Fellow, IEEE)

[1]School of Electronic Engineering, Xidian University, Xi'an 710071, China
[2]School of Life Science and Technology and School of International Education, Xidian University, Xi'an 710071, China
[3]School of Computer Science and Technology, University of Bedfordshire, Luton LU1 3JU, U.K.
[4]Northwest Women's and Children's Hospital, Xi'an Jiaotong University, Xi'an 710061, China
[5]School of Life Science and Technology, Xidian University, Xi'an 710126, China
[6]Institute of Automation, Chinese Academy of Sciences, Beijing 100190, China

CORRESPONDING AUTHOR: J. TIAN (jaytian99@gmail.com)

This work was supported in part by the National Natural Science Foundation of China under Grant 61671349, in part by the Fundamental Research Funds for the Central Universities, and in part by the International Scientific and Technological Cooperation and Exchange Projects in Shaanxi Province under Grant 2017KW-005.

ABSTRACT Essential tremor (ET) is a neurological disorder characterized by rhythmic, involuntary shaking of a part or parts of the body. The most common tremor is seen in the hands/arms and fingers. This paper presents an evaluation of ETs monitoring based on finger-to-nose test measurement as captured by small wireless devices working in shortwave or *S*-band frequency range. The acquired signals in terms of amplitude and phase information are used to detect a tremor in the hands. Linearly transforming raw phase data acquired in the *S*-band were carried out for calibrating the phase information and to improve accuracy. The data samples are used for classification using support vector machine algorithm. This model is used to differentiate the tremor and nontremor data efficiently based on secondary features that characterize ET. The accuracy of our measurements maintains linearity, and more than 90% accuracy rate is achieved between the feature set and data samples.

INDEX TERMS *S*-band sensing technique, essential tremor, biomedical engineering.

I. INTRODUCTION

Eessential tremor (ET) is one of the common neurological conditions that affect parts of the body and steadiness. ET affects the steadiness causing an oscillatory movement that is measurable. Around 30% of patients are misdiagnosed as Parkinson's disease or other diseases. A reason for an onset of ET is age, the prevalence increases with an increase in age. ET reaches 12% in incidence for patients who are older than 70 years. Studies have shown that ET is one kind of autosomal dominant disease. Gulcher *et al.* [1] found that the virulence gene for ET is located at "3q13" in [2]; it was also discovered that the virulence gene is also located at "2p22-25." ET is one kind of central tremor; caused by the abnormal vibration of the network structure in the central nervous system. The clinical manifestation of ET effect is the upper extremities of the body causing disruption of daily activities.

Tremor mode of ET can be divided into postural tremor and action tremor; in most cases, patients suffering from either of these, face difficulties in being steady and ability to control while performing physical tasks. Usually, the frequency of the tremor is 4-12 times per second; the tremor frequency for each patient is basically fixed. Typical ET mainly happens on the upper limb, head, lower limbs, and trunk. The most common locations are hands and upper limbs. Bain *et al.* [3] and Elble [4] proposed the core diagnostic criteria of ET are: action tremor of hands, forearm and head tremor without dystonia. They also presented some minor diagnostic criteria such as a positive family history. Exclusion criteria are also included: hyper-thyroid tremor, primary orthostatic tremor, target specific tremor, etc. Pain experienced by patients due to this disease is very important to detect this kind of disease at an early stage.

This work primarily considers symptoms related to ET. In disease detection process, we mainly considered the postural tremor with a single symptom. In other words, the symptom that is most obvious when the subject maintains a certain posture. For some patients, the tremor may become more

serious when they are in motion while others might tremble at the very beginning of the movement. It is worth mentioning that the tremor seldom occurs when the subjects are stationary. The tremor usually starts from one side of the hand, and then it might extend to the upper limb. The frequency of 4-12Hz range varies with age, studies have shown it decreases with increasing age [5]. There are some other symptoms which are related to ET, such as dystonia, hereditary cerebellar ataxia, and classic migraine that are out of the scope of this work. Currently, the confirmatory methods of ET are still controversial and they mainly depend on the medical history and clinical features. By considering the diagnostic criteria of ET, we aim to characterize the features of the tremor and postures as concisely as possible. The effectiveness of the nose-target hand movement experiment has been demonstrated in [5] and can be considered as a diagnostic test. By exploring the time and spatial information of the wireless signals, the key features of the disease were found. This technique makes it easy, relatively simple and an important tool for diagnosing ET.

The paper is organized as follows: Section II presents the related work, section III gives the basic theory of the S-band sensing technique leveraging wireless channel information (WCI); Section IV gives the details of the experiment, and section V provides the data classification and section VI draws a conclusion.

II. RELATED WORK

Several researchers have introduced methods detecting the ET disease. Thanvi *et al*. [6] argued that the essential tremor provides a frequency between 4 to 12 Hz with varying amplitude that depends on the magnitude of the stress, voluntary body motions, and posture. The frequency of ET patients is higher in subjects without ET. Ahlrichs and Samà [7] introduced a system leveraging acceleration data obtained from subject's wrist and classified tremors and non-tremors. Other studies such as [8], [9], and [10] used various kinds of tremor data obtained using acceleration sensors to identify the tremors. However, most of the systems exploit specialized hardware that makes it expensive solution and is mostly applicable in a laboratory environment.

III. FUNDAMENTALS OF WIRELESS CHANNEL INFORMATION

It is well known that the received signal strength indicator (RSSI), is used to obtain the average of the multipath signals for wireless measurement. Generally, due to the rich multipath effect, it is not appropriate to consider RSSI for indoor sensing. It has been demonstrated that the RSSI readings of a stationary receiver present some fluctuations. In a typical indoor environment, the signal at the receiving side is the superposition of signals from multiple paths; for each path, the time delay, fading and phase shift are different. RSSI can be represented as:

$$RSSI = 10\log_2\left(\|V\|^2\right) \tag{1}$$

'V' is the voltage level measured based on the RF input signal; time variation at a position will cause changes in the relative RSSI. A small change in a certain component will cause a significant change in the phase information leading to the fluctuation of the RSSI. It is noticeable that in an indoor environment, the distance and RSSI do not follow a strict monotonous relation; hence it is possible to get a higher RSSI value at the more distant location. Since RSSI only provides information in medium access control, it is very important to explore the wireless channel characteristics including fine-grained information.

The wireless channel information (WCI) has many advantages over RSSI. The WCI estimates the channel information for each subcarrier and characterizes the frequency selective fading. In addition, it contains the amplitude and phase information for each subcarrier. The proposed method uses amplitude and phase information of the WCI measurement provided in the S-Band frequency range. When a moving obstacle is present given the wireless range, WCI registrations constantly change due to the variances in the wireless signals. These perturbations of the wireless signal or multipath propagation effects such as reflection, refraction and delay distortion are measured and analyzed.

To fully characterize the wireless channel, we consider it a system that is analyzed as an impulse response h (τ) in time domain as shown in equation (2)

$$h(\tau) = \sum_{i=1}^{N} \alpha_i e^{-j\theta_i} \delta(\tau - \tau_i) \tag{2}$$

where α_i, θ_i and τ_i are the magnitude, phase and time delay of the i^{th} path respectively; N is the number of paths and $\delta(\tau)$ is the Dirac delta function; each pulse represents the number of multipaths for every time delay.

Wireless channel in the frequency domain is represented as a superposition of phase and frequency of signals. The reflections or selective fading of signals are captured by the antenna and with appropriate signal conditioning, we obtain the amplitude and phase. This is collectively called as channel frequency response (CFR) that represents the magnitude of the signal that has delay profile and power spectral density. The CFR values constitute amplitude and phase spectrum for a set of 30 sub-carriers. Thus, both signal variation of small multipath response together is widely applied to channel characterization. In the time domain, the received signal $r(t)$ is the convolution between transmitting signal $s(t)$ and channel impulse response $h(t)$ given as shown below

$$r(t) = s(t) * h(t) \tag{3}$$

In the frequency domain,

$$R(f) = S(f) \times H(f) \tag{4}$$

Convolving the received and transmitting signal we obtain the CFR, that is the rate between the transmitting and receiving signal. For an approximated flat power spectrum, we can

IEEE Journal of Translational Engineering in Health and Medicine

approximate equation (4) and take the inverse Fourier transform as shown in equation (5) [11]:

$$h(t) = \frac{1}{P_S}\xi^{-1}\left\{S^*(f)\,R(f)\right. \tag{5}$$

where ξ^{-1} is the inverse Fourier transform, $R(f)$ is the Fourier transform of the receiving signal, $S^*(f)$ is the complex conjugate of the Fourier transform of the transmitting signal, and P_S is the power of the transmitting signal.

Using the toolchain provided by the interface card, a channel frequency response can be obtained in the form of wireless channel information.

The channel model in the frequency domain can be written as

$$Y = H \times X + N \tag{6}$$

where Y represents the received signal in frequency domain, H is the channel frequency response, N is the noise vector and X is the transmitted signal (frequency domain).

The system is multicarrier and the spacing of frequencies that is transmitted is based on Orthogonal Frequency Division Multiplexing (OFDM). Here the 30 subcarriers are orthogonally spaced to transmit and receive the perturbed signals using the network interface card. For each subcarrier, amplitude and phase information can be found.

$$\vec{H}(f_i) = \vec{H}(f_i)\; e^{j\sin\left\{\angle\vec{H}(f_i)\right\}} \tag{7}$$

where $\vec{H}(f_i)$ is the WCI for the subcarrier with a central frequency of f_i and $\angle\vec{H}(f_i)$ is the amplitude. WCI characterizes the fine-grained time and spectrum structure for the wireless channel. One CFR packet can be written in the form of WCI as:

$$\vec{H} = \left[\vec{H}(f_1), \vec{H}(f_2), \ldots, \vec{H}(f_i), \ldots, \vec{H}(f_N)\right]^T, \quad i \in [1, 30] \tag{8}$$

The WCI phase information is extremely random due to random noise and unsynchronized timing between the transmitter-receiver pair. In this work, we use the calibrated phase information as discussed in [12].

$$\psi_j' = \psi_j - 2\pi \times \frac{\eta_i}{N} \times \varsigma + \mu + P_n \tag{9}$$

where ψ_j' is the random phase, ς is the offset timing of the network interface card and μ is the unknown phase offset.

IV. NOSE-TARGET HAND MOVEMENT EXPERIMENT

According to the Washington Heights-In Wood Genetic Study of ET (WHIGET) [14], nose-target hand movement experiment is one of the most common test methods to evaluate ET. The experiment was carried out in an enclosed room to minimize the impact of the surrounding environment on the radio wave in S-Band. The thickness of the material was carefully selected to ensure that its reflectivity for a vertical wave at the corresponding wavelength can satisfy the experimental requirement. The experiment was performed as given in figure 1.

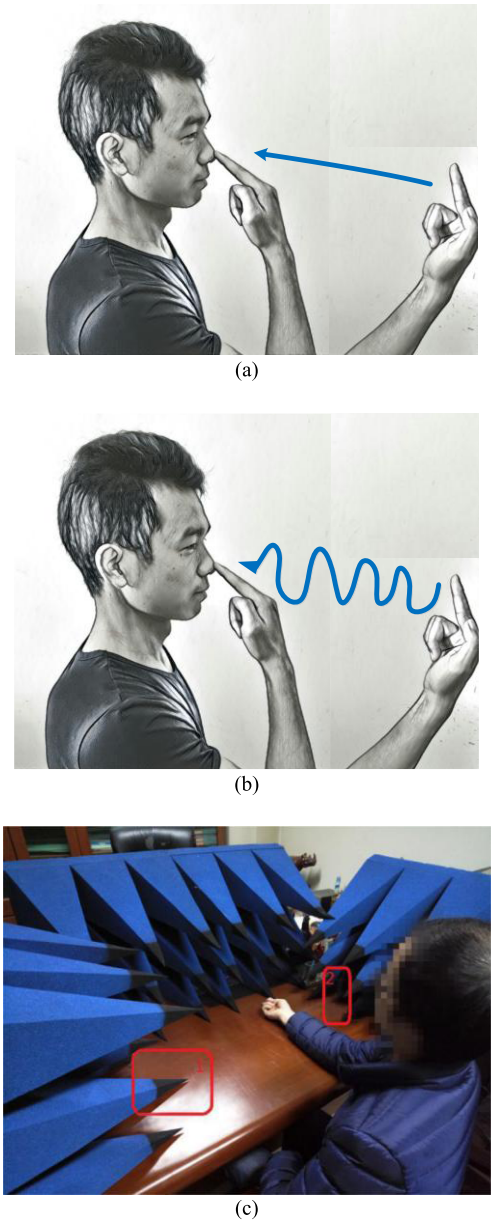

FIGURE 1. Finger-to-nose Test and the detection of ET. (a) Finger-to-nose Test sketch map (without ET). (b) Finger-to-nose Test sketch map (with ET). (c) Finger-to-nose Test measurement.

The specific motion requirement for the subject is: first, the subject puts his forearm on the table horizontally; second, he lifts his forearm slowly, touches his nose with the index finger; then, he puts his forearm on the table slowly to finish one cycle of movement as part of the experiment. To improve our confidence about the conclusions drawn, the experiments were repeated many times for 8 various subjects.

A. SUBJECT RECRUITMENT FOR DATA COLLECTION

Eight subjects (four patients suffering from essential tremor disease) as shown in table 1, volunteered to assess the

TABLE 1. Details for eight subjects.

ID	Gender	Weight (kg)	Height (cm)	Disease (ET)
1	Male	71	172.0	Yes
2	Male	80	175.1	Yes
3	Female	60	160.9	Yes
4	Female	62	162.4	Yes
5	Male	75	176.2	No
6	Male	84	174.3	No
7	Female	61	159.5	No
8	Female	64	160.3	No

proposed method. The reason for selecting the ET patients and normal persons (without ET) was to examine the difference between the data obtained from volunteers with and without ET.

The patients suffering from ET did not take any medication four hours prior to the experiment.

It was made sure that no external movements should be experienced when the data is being recorded since the surrounding motions around the experimental setup will affect the measured data.

Our system uses a wireless device, and S Band directional antenna that continuously monitors the patient in an indoor environment. We aim at non-invasive and easy deployment system for data acquisition. The above-stated tests are compared with subjects who do not have ET versus subjects who do have tremors. The subject not suffering from ET is able to perform the test smoothly with no tremors recorded. While subject with ET, due to the conditions have recoded tremors while moving the hand from the nose to the table and back. The measurements clearly show the perturbations in the S-band as seen in the amplitude and phase information. These signals are pre-processed and seamlessly recorded using WCI tool-chain.

The following figures give the raw CFR information. For comparison, a subject without ET was also considered.

Figure 2(a) shows the variances of raw channel frequency response data obtained during the experiment. Each packet comprises of 30 subcarriers as seen in the x-axis and the corresponding amplitude in dB on the y-axis. For the current study, we have chosen the nineteenth sub-carrier of the CFR stream. In figure 2(b) it is clear that the amplitude of the nineteenth sub-carrier fluctuates smoothly, but the range of the amplitude is very limited (20-25dB). The amplitude cycle is completed in 55 packets or over a time period of 5.5 seconds, and the difference between the higher trough and lower trough is around 1.5dB. This 1.5dB is attributed to the minute movements in the surroundings such as reflection from the ceiling, the breathing of the subject, etc. With the subject having ET, the variations in raw CFR values is as seen in figure 2(c).

Comparing the graphs in figure 2(a) and 2(c) we notice that the peaks are more pronounced that is the baseline to differentiate the normal versus perturbation in the S-band signals. This double-dip is seen in graph 1(c) marks the choice

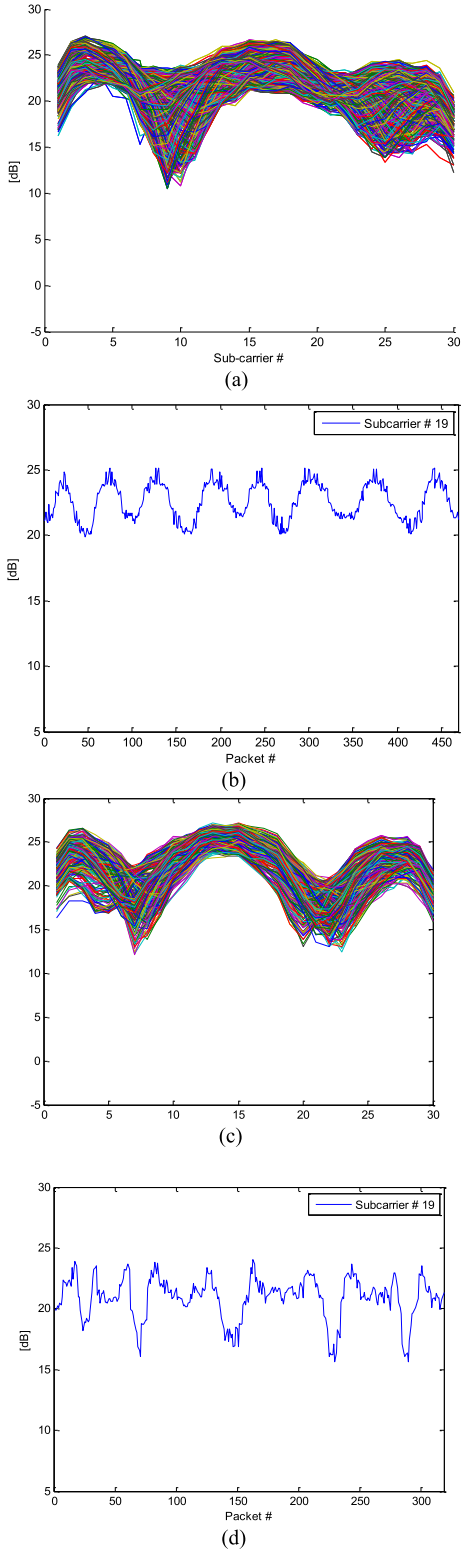

FIGURE 2. The variances of amplitude information obtained during the experiment. (a) The raw CFR data recorded for a person without ET. (b) Time history for the person without ET. (c) The raw CFR data recorded for the person with ET. (d) Time history for the person with ET.

in subcarrier for monitoring and analyzing our recorded data. In order to make specific analyze of variations in amplitude versus time history, we consider figure 2(d). Here, data

IEEE Journal of Translational Engineering in Health and Medicine

acquisition is done for a period of 33 seconds. The amplitude information fluctuates in an irregular manner between 15 dB and 24 dB for 330 packets.

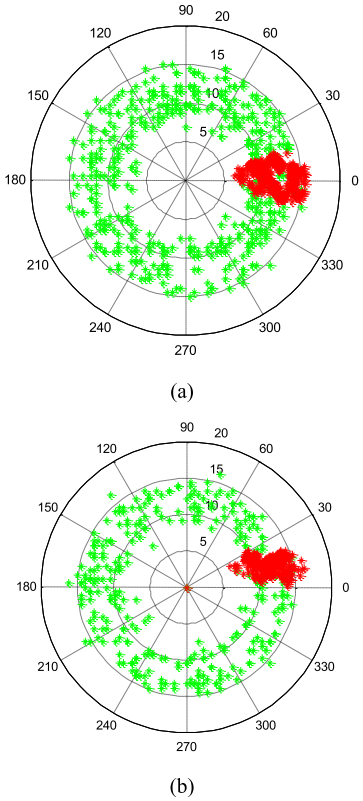

FIGURE 3. Phase information obtained for detecting ET. (a) Phase information before and after linear transformation (subject without ET). (b) Phase information before and after linear transformation (subject with ET).

We further analyze the calibrated phase information for the person with ET and without ET. Here as seen in figure (3) the polar plots give a better indication. The phase variations are close to zero in the case of the subject without ET. While as seen in figure 3(b) the phase shift is observed and is an important factor. This phase change coupled with amplitude measured will provide the rigorous movement indicator as against the normal subject movement that is linear. Thus, the characterization of such non-linear and movement disorders such as ET can be analyzed using phase information too.

Figure 3 (a) and (b) illustrate the calibrated phase information for the subject with ET and without ET. Figure 3(a) shows that the calibrated phase information in *red color* varies between 10 to 15 dB and from 15° to 350°. On the other hand, the calibrated phase information as seen in figure 3(b) shows 7 to 16 dB between 0° to 30° of a subject suffering from ET.

B. SUPPORT VECTOR MACHINE FOR CLASSIFICATION

As seen in figure1 (a) and 1 (c) the amplitude measurements are not too discriminate. Hence to categorically look at the human condition as normal versus ET we look at amplitude information against time history and calibrated phase information using the support vector machine.

The advantage of SVM over other machine learning algorithms such as random forest [15], neural networks [16], and K-nearest neighbor [16] is that it can achieve high efficiency considering the practical problem and the inner-product kernel function resolving the linearly non-separable data points in a higher-dimension-space [17]. Support vector machine (SVM) is used to classify two sets of data. A decision boundary called hyperplane separates both classes. Using SVM algorithm we optimize the data points that are used to predict the class of newly acquired signals. Detecting the outliers and computing the feature set for a new set of acquired data and associated with the corresponding class is efficiently done using SVM.

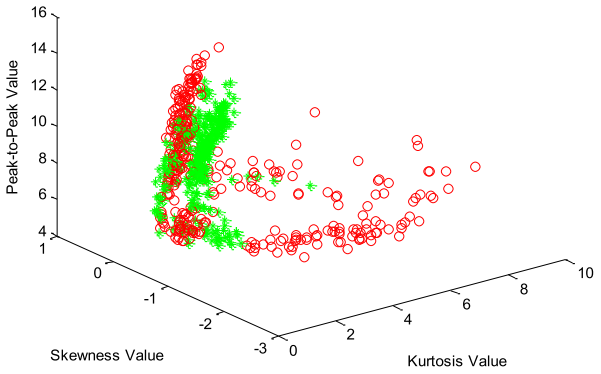

FIGURE 4. Feature space results for the two cases; indicators are kurtosis value, skewness value, and peak-to-peak value.

The features we have used are peak-to-peak value, kurtosis, and skewness. The three features are computed as shown in equation (10) to (12). In a set of possible SVM features, we considered kurtosis values, skewness value, and peak-to-peak values as the best performers in our case as shown in figure 4

$$F_{PPV} = \max(c) - \max(c) \tag{10}$$

$$F_{KV} = \frac{1}{P}\sum_{i=1}^{P}\left[\frac{c_i - \mu_c}{\sigma}\right]^4 \tag{11}$$

$$F_{SV} = \frac{1}{P}\sum_{i=1}^{P}\left[\frac{c_i - \mu_c}{\sigma}\right]^3 \tag{12}$$

F_{PPV}, Peak-to-peak value is the measure of amplitude per packet while F_{KV} and F_{SV} are the statistical features collective for a packet. These two features define the shape and symmetry of the data. A relative comparison of the three features and their interdependency in the feature space is shown below.

Initially, the goal was to identify a limited number of SVM features that would serve as a blueprint for WCI data. A large number of possible SVM features were defined, among which the optimum features were computed using MATLAB. Figure 4 describes the signals acquired or CFR data as shown in terms of data points in the green and red

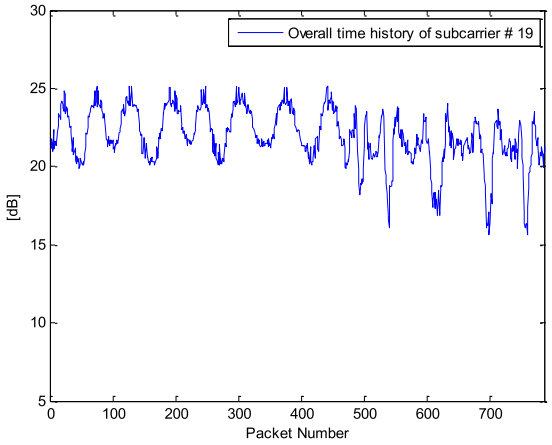

FIGURE 5. The overall time history of person with and without ET.

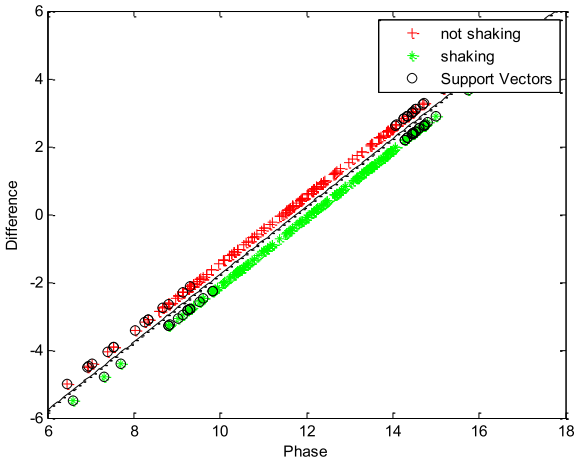

FIGURE 7. The differences between phase information values and mean phase values.

circles representing the non-ET and ET respectively. Comparing the ET and non-ET feature sets as seen in figure (4) the closeness resulting our classification methods provide us an accuracy rate. Single carrier observations:

Figure 5 shows the overall time history of 2 scenarios of subjects without ET and with ET. Over a period of time when measurements where done in the experimental mentioned above, we can observe the amplitude variations.

Based on the data, fluctuations of amplitude fluctuation around 1dB, or measured values of 24 to 25 dB was observed. The variance of around 4dB is observed for subjects with ET. As shown in figure (5), from 0 to 450^{th} packet with the variance of amplitude (in dB) around ± 4 is the acquisition for a subject suffering from ET. From 450^{th} to 780^{th} packet, with a variance of $\cong 1$ is for a subject who does not have tremors while having a steady movement.

We further classify the two datasets, one for ET and another for non-ET using SVM as in figure 6.

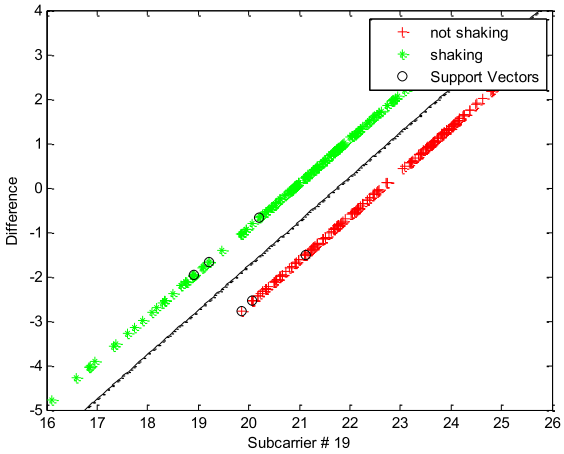

FIGURE 6. Difference between the amplitude values and mean values for subcarrier 19.

With a clear hyperplane as a decision boundary, we observe the support vectors in either side, indicating a linearly separable data set. Figure 6 indicates the SVM results obtained when the amplitude levels for subcarrier 19 that were chosen for classification. A high accuracy was achieved considering the individual subcarrier.

Next, we analyze the results obtained when the calibrated phase information is considered. The choice of features such as peak-to-peak, skewness, and kurtosis give the best set of the description of a packet data or 30 sub-carriers.

Comparing figure (6) and (7) we can deduce that the hyperplane boundary defines the classification more precisely with least bias error. An accuracy of 99 % was achieved when the sanitized phase information was classified considering the tremors and non-tremors.

V. CONCLUSION

Essential Tremor is a progressive disease that affects patients' quality of life. Detection and treatment at an early stage are therefore very important since it hampers everyday activity of the patient. Traditionally, ET can be evaluated by using neuroimaging techniques, genetic techniques, and EMG. In this study, we consider the motor symptoms of ET and apply the non-contact approach to detect ET. With a non-invasive, we observe that it can effectively monitor the interference and influence in the subjects' gait or walk. By comparing the amplitudes and sanitized phase information for ET and non-ET subjects, it is found that the ET subject has huge fluctuations in the amplitude and the difference between the lower trough and higher trough is about 4dB, thus the cycle is not as stable as in case of the non-ET subject. The calibrated phase information also provides an accuracy rate of more than 90 % when the data points for ET and non-ET are classified using SVM. Comprehensively using SVM and computing peak-to-peak, skewness and kurtosis we automate the detection of the tremor. The results can be extended to larger setup or group of people since non-contact technique can effectively detect ET or non-ET movements. Thus, non-invasive monitoring is significant for early treatment and monitoring of such sporadic episodes and managing medication for such conditions.

IEEE Journal of Translational Engineering in Health and Medicine

ACKNOWLEDGMENT

The authors would like to thank Northwest Women's and Children's Hospital of Xi'an Jiaotong University for their help and guidance.

REFERENCES

[1] J. R. Gulcher *et al.*, "Mapping of a familial essential tremor gene, *FET1*, to chromosome 3q13," *Nature Genet.*, vol. 17, pp. 84–87, Sep. 1997.

[2] J. J. Higgins, L. T. Pho, and L. E. Nee, "A gene *(ETM)* for essential tremor maps to chromosome *2p22-p25*," *Movement Disorders*, vol. 12, no. 6, pp. 859–864, 1997.

[3] P. Bain *et al.*, "Criteria for the diagnosis of essential tremor," *Neurology*, vol. 54, p. S7, Jun. 2000.

[4] R. J. Elble, "Diagnostic criteria for essential tremor and differential diagnosis," *Neurology*, vol. 54, pp. S2–S6, Jan. 2000.

[5] W. C. Koller, K. Busenbark, and K. Miner, "The relationship of essential tremor to other movement disorders: Report on 678 patients," *Ann. Neurol.*, vol. 35, no. 6, pp. 717–723, 1994.

[6] B. Thanvi, N. Lo, and T. Robinson, "Essential tremor—The most common movement disorder in older people," *Age Ageing*, vol. 35, no. 4, pp. 344–349, 2006, doi: 10.1093/ageing/afj072.

[7] C. Ahlrichs and A. Samà, "Is 'frequency distribution' enough to detect tremor in PD patients using a wrist worn accelerometer?" in *Proc. 8th Int. Conf. Pervasive Comput. Technol. Healthcare (ICST)*, Oldenburg, Germany, 2014, pp. 65–71.

[8] S. Patel *et al.*, "Using wearable sensors to predict the severity of symptoms and motor complications in late stage Parkinson's disease," in *Proc. 30th Annu. Int. Conf. IEEE Eng. Med. Biol. Soc. (EMBS)*, Vancouver, BC, Canada, Aug. 2008, pp. 3686–3689.

[9] D. J. Wile, R. Ranawaya, and Z. H. Kiss, "Smart watch accelerometry for analysis and diagnosis of tremor," *J. Neurosci. Methods*, vol. 230, pp. 1–4, Jun. 2014, doi: 10.1016/j.jneumeth.2014.04.021.

[10] C. Thanawattano, C. Anan, R. Pongthornseri, S. Dumnin, and R. Bhidayasiri, "Temporal fluctuation analysis of tremor signal in Parkinson's disease and essential tremor subjects," in *Proc. 37th Annu. Int. Conf. IEEE Eng. Med. Biol. Soc.*, Aug. 2015, pp. 6054–6057.

[11] K. Qian, C. Wu, Z. Yang, Y. Liu, and Z. Zhou, "PADS: Passive detection of moving targets with dynamic speed using PHY layer information," in *Proc. 20th IEEE Int. Conf. Parallel Distrib. Syst. (ICPADS)*, Hsinchu, Taiwan, Dec. 2014, pp. 1–8.

[12] S. Sen, B. Radunovic, R. R. Choudhury, and T. Minka, "You are facing the Mona Lisa: Spot localization using PHY layer information," in *Proc. ACM MobiSys*, 2012, pp. 183–196.

[13] E. D. Louis, "Essential tremor," *Lancet Neurol.*, vol. 4, no. 2, pp. 100–110, 2005.

[14] H. Nakahara, A. Jinguji, S. Sato, and T. Sasao, "A random forest using a multi-valued decision diagram on an FPGA," in *Proc. IEEE 47th Int. Symp. Multiple-Valued Logic (ISMVL)*, Novi Sad, Serbia, May 2017, pp. 266–271.

[15] O. J. L. Castro, C. C. Sisamón, and J. C. G. Prada, "Bearing fault diagnosis based on neural network classification and wavelet transform," in *Proc. 6th WSEAS Int. Conf. Wavelet Anal. Multirate Syst.*, Bucharest, Romania, Oct. 2006, pp. 22–29.

[16] J. Tian, C. Morillo, M. H. Azarian, and M. Pecht, "Motor bearing fault detection using spectral kurtosis-based feature extraction coupled with K-nearest neighbor distance analysis," *IEEE Trans. Ind. Electron.*, vol. 63, no. 3, pp. 1793–1803, Mar. 2016.

[17] S. T. Dumais, "Using SVMs for text categorization," *IEEE Intell. Syst.*, vol. 13, no. 4, pp. 21–23, Jul. 1998.